The ice-like water monolayer near the wall makes inner water shells diffuse faster inside a charged nanotube

Xiaoyan Zhou, Chunlei Wang, Fengmin Wu, Mei Feng, Jingyuan Li, Hangjun Lu, and Ruhong Zhou

Citation: The Journal of Chemical Physics **138**, 204710 (2013); doi: 10.1063/1.4807383
View online: http://dx.doi.org/10.1063/1.4807383
View Table of Contents: http://scitation.aip.org/content/aip/journal/jcp/138/20?ver=pdfcov
Published by the AIP Publishing

The ice-like water monolayer near the wall makes inner water shells diffuse faster inside a charged nanotube

Xiaoyan Zhou,[1,2] Chunlei Wang,[3] Fengmin Wu,[1,2] Mei Feng,[1] Jingyuan Li,[4] Hangjun Lu,[1,a)] and Ruhong Zhou[5,6,a)]

[1]*Department of Physics, Zhejiang Normal University, Jinhua 321004, China*
[2]*Department of Physics and Institute of Theoretical Physics, Shanxi University, Taiyuan 030006, China*
[3]*Shanghai Institute of Applied Physics, Chinese Academy of Sciences, Shanghai 201800, China*
[4]*Institute of High Energy Physics, Chinese Academy of Sciences, Beijing, China*
[5]*Computational Biology Center, IBM Thomas J. Watson Research Center, Yorktown Heights, New York 10598, USA*
[6]*Department of Chemistry, Columbia University, New York, New York 10027, USA*

(Received 21 January 2013; accepted 23 April 2013; published online 30 May 2013)

Using molecular dynamics simulations, we have investigated the impact of the ice-like water monolayer inside the tube and nearest to the tube wall on the diffusion properties of other inner water shells confined within a charged nanotube. We find that the axial diffusion coefficient of the first water monolayer near the wall monotonously decreases with the charge size on the nanotube, indicating a tighter control of the first monolayer from the larger sized charge. However, for the other water shells, the diffusion coefficients increase when the charge is larger than a critical value q_c ($\sim$1.0 e). This unexpected phenomenon is attributed to the decreased number of hydrogen bonds between the first monolayer and other inner water shells caused by the very unique hydrogen-bond network patterns in the first ice-like monolayer, which makes it behave like a "hydrophobic water layer." Our findings may have implications for water treatment, non-fouling surfaces, catalysis engine, and biological sensor. © *2013 AIP Publishing LLC*. [http://dx.doi.org/10.1063/1.4807383]

I. INTRODUCTION

Water layers at the surface often exhibit unique properties and have crucial influences on interfacial properties.[1–8] For example, water shell close to vicinity of a protein/enzyme is central to the stability of the structure, conformation, and the biological function. Almost all biological macromolecules are inactive in the absence of water.[9] Water monolayer on mica surfaces has an ice-like characteristic because of its longer relaxation time as compared to bulk liquid water.[10] Ice monolayers on metal surfaces have hydrophobic-like property due to the fact that no dangling OH bonds exist in the ice monolayer, which itself features a two-dimensional hydrogen bond network.[11–13] So, a molecular-level understanding of the structure and dynamics of such water layers at surface is fundamental to physics, chemistry, and biology.[14,15]

Recently, "water that does not wet a water monolayer" (i.e., hydrophobic water layer) at room temperature has been recently observed from both experiments[16,17] and simulations.[18–22] This unexpected phenomenon is attributed to the structure of the ordered water monolayer at the substrate.[20] The substrate of the previous work has a planar hexagonal structure of neighboring bond lengths of 0.142 nm, which is similar to the graphene surface. The appropriate atomic partial charge quantity and unique distribution pattern account for the hydrophobic-like water layers. Then, an interesting question arises: if such a substrate is rolled up into a nanotube, how does the structure of the water monolayer near the curved wall affect the properties of inner water layers now confined with the nanotube?

Many studies have shown that the properties of water confined inside carbon nanotubes or narrow pores (sub 2-nm in diameter) differ from bulk water, such as the ordered water structure, non-Fickian-type diffusion, and ultra-fast motion of water molecules, and so on.[23–32] Among all the properties of water inside nanotubes, diffusion plays a key role in defining other properties such as viscosity, permeability, flow type, and convection heat transfer.[33,34] Several studies were performed to investigate the diffusion properties of water inside the carbon nanotubes (CNTs). Striolo discussed the mechanism of water diffusion inside a narrow CNT.[35] Liu *et al*. studied the effects of CNT diameter, density of water, and temperature,[36,37] as well as the topology (armchair CNT vs. zigzag CNT),[38] on the diffusion property of water. Very recently, Aluru and co-workers further investigated the spatial variation of diffusion in CNTs with different diameters and analyzed the diffusion types in different regions of CNT.[34] They observed a diffusion enhancement near the CNT wall and provided reasoning on why carbon nanotubes are fast transporters of water.[39] This result is due to the reduced number of water hydrogen bonds near the wall, which provides less restriction and more freedom for the water molecules near the tube wall.

Carbon nanotubes have various applications in nanofluidics including channels, sensors, filters, and nano-devices for drug delivery. CNTs exhibit the potential to be the drug carriers, functional group is crucial for the CNT to achieve targeting and become more soluble and serum-stable. However, the

a)Authors to whom correspondence should be addressed. Electronic addresses: zjlhjun@zjnu.cn and ruhongz@us.ibm.com.

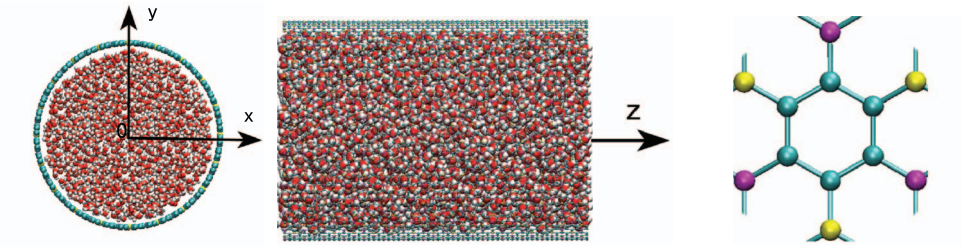

FIG. 1. (a) Side view and (b) front view of the simulation framework. (c) Geometry of the nanotube model. Yellow and purple spheres represent negative and positive charges, respectively, while the green represents the neutral solid atom.

impact of functional group on the behavior of water molecules within CNT is still elusive. We designed the model system, in which the carbon nanotube is charged, to study the behavior of water molecules in this regards, and the charge distribution is based on our previous work.[20] In this paper, we investigate the effect of water monolayer nearest to the charged wall on the diffusion property of inner water layers confined within a charged nanotube using molecular dynamics simulations. Conventionally, the charges and/or dipoles on the substrate (solid wall) will lead to hydrophilicity of solid wall. The diffusion coefficient of water near the wall will decrease with the increase of the charge value. However, we find that the wall hydrophilicity is also related to topography of the charges on the solid wall. Water molecules nearest to the wall can form a well-ordered ice-like water monolayer due to the unique charge-water interaction. The diffusion coefficients along the axial direction in nanotubes are computed. The axial diffusion coefficient of the first water layer near the nanotube wall decreases dramatically when the charge value increases. Interestingly, for the other water shells, the diffusion coefficients increase when $q > q_c = 1\ e$. The mechanism behind the phenomenon can be explained by the hydrogen bonds between water shells.

II. MODEL AND KEY PARAMETERS

The simulation framework is shown in Figure 1. The model nanotube has the same hexagonal structure of the (40, 40) carbon nanotube with 5.346 nm diameter. Positive and negative charges of the same magnitude q were assigned to atoms located diagonally in neighboring hexagons. It should be noted that this is just a model system with relatively large charges for simulation purpose. In practice, one might assign these charges by attaching functional groups such as –COO– and $–NH_3^+$ to the single-walled or multi-walled carbon nanotubes,[40–42] with both existing and potential new materials.[20,43] Overall, the modeled nanotube is neural. There are 4572 water molecules confined inside it.

Our simulations were performed using a time step of 2.0 fs with the GROMACS 4.0.7 in an *NVT* ensemble. Temperature was maintained at 300 K using Nose-Hoover thermostat. All the parameters were taken from our previous work.[21] The carbon atoms of the nanotube are represented with Lennard-Jones (LJ) parameters $\epsilon_{ss} = 0.105$ kcal/mol, $\sigma_{ss} = 3.343$ Å. The SPC/E water model and GROMOS43a1 force fields were used.[44] Here, we use ϵ_{ss} and σ_{ss}, not using ϵ_{cc} and σ_{cc}, to emphasize the model system, not the realistic system. S represents solid. This parameter is based on our previous research work.[20] In this way, there is no dispersion interaction between hydrogen atoms in SPC/E water model and carbon atoms. Ma *et al.* shows that none of the functionals considered provide a satisfactory description of the water-graphene interaction, unless dispersion forces are accounted for.[45] Meanwhile, we focus on the impacts of charge distribution of the nanotube on the water behavior and the corresponding mechanism in this work. A periodic boundary condition was applied in the axial direction (z) and the simulation box size was $10 \times 10 \times 7.518$ nm^3. The cutoff distance for the LJ interactions is 15 Å. The long-range electrostatic interactions were computed by using the particle mesh Ewald method (real space cutoff, 10 Å; reciprocal space gridding, 1.2 Å, fourth-order interpolation). For simplicity, the carbon atoms were frozen to their lattice position. Previous molecular dynamics studies on nanofluidic properties of CNTs under equilibrium conditions have shown that treating CNTs as rigid in their lattice is a reasonable approximation.[34,35,46,47]

III. RESULTS AND DISCUSSION

Figure 2 shows the radial density profiles of the water in the nanotube with different q. The radial density $\rho(r)$ is defined as the ratio of local water density at r to the water density at the center region. The local densities are calculated by dividing the water liquid into many cylindrical shells

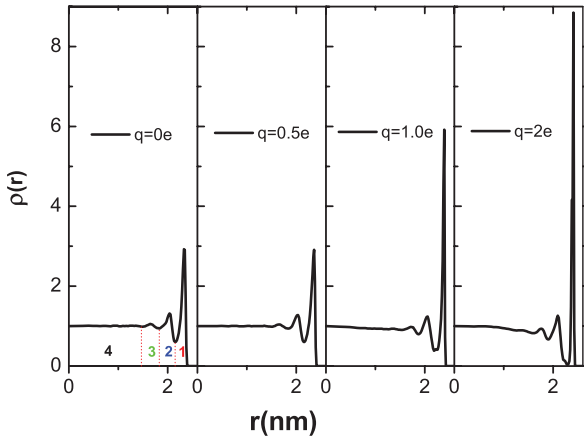

FIG. 2. Radial density profiles of the water in the nanotubes for different q and r is the distance from the center of the nanotube.

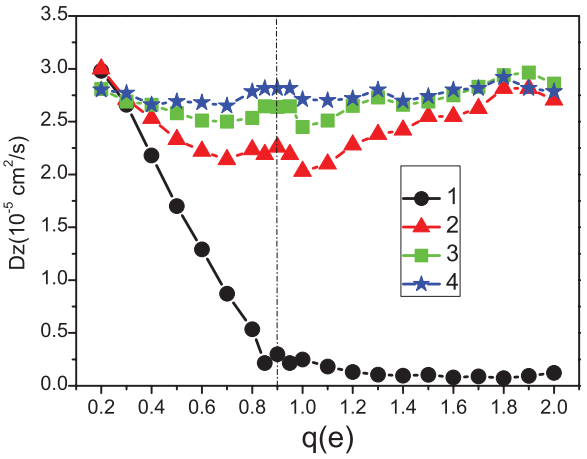

FIG. 3. The axial diffusion coefficient for different shells.

in the r direction, then taking the statistical average for the density for each shell. Here, we used the coordinate of oxygen of water molecules to calculate the density profile. From Fig. 2, it is obvious that there is dense water monolayer near the tube wall for both the neutral and charged nanotubes (the first sharp density peak near the nanotube wall). In the center region of the nanotubes, unlike the small sized nanotubes, the water molecule distributions are uniform. As the charge q increases, the first density peak becomes sharper and sharper with higher and higher amplitude, indicating that the first water monolayer near the tube wall becomes more and more ordered. Meanwhile, due to the strong attractive force between the charged wall and water molecules, the water monolayer shifts towards the tube wall slightly as well. For easy discussion, we divide the inner confined water into four shells total, according to the distribution of water density (see Fig. 2, $q = 0e$). Note that the region sizes of the first, the second, and the third shell are about the size of one water molecule (about 3.8 Å), while the fourth shell is much larger and also further away from the tube wall. In fact, we can view the fourth shell as the bulk-like region.

To further investigate the effect of the charged wall on the axial diffusion coefficient of water inside the nanotube, we computed the axial diffusion coefficients for these four shells, denoted by $D_{z(n)}$ ($n = 1, 2, 3, 4$). The simulation results are shown in Fig. 3. When the charge value is small ($q < 0.3e$), the axial diffusion coefficient near the tube wall (D_{z1} and D_{z2}) is ~10% larger than that of the center region (D_{z3} and D_{z4}), consistent with the result of Aluru and co-workers.[33] In the first shell, due to the attraction of the charges, the axial diffusion coefficient decreases dramatically as q increases to $0.9e$, and then decreases slowly to nearly zero with further increasing of q. The axial diffusion coefficient of the water molecules in the first shell is so small that these water molecules are essentially frozen in the tube when $q > 0.8e$. They form an ice-like water monolayer (see Fig. 4). The axial diffusion coefficients in the 2nd and 3rd shells decrease, in general, in the charge interval of $0e$-$0.7e$. However, they increase for $q > 1.0e$. However, for the 4th shell, the axis diffusion coefficient is about 2.71 (10^{-5} cm^2/s) with little fluctuation.

Then how to explain this unexpected increase in the diffusion coefficients? We have found that the ordered first water monolayer near the nanotube wall is responsible for this abnormal diffusion property. Different from the structure of "ice nanotube" inside the (14,14), (15,15), (16,16) CNTs, reported by Koga *et al.*,[25] here, a hexagonal ice monolayer is formed near the charged nanotube wall as shown in the right panel of Figure 4. There are two typical configurations for water molecules. Water molecules in A-type state have both –OH pointing towards the 2 neighboring water molecules, tending to form two hydrogen bonds. Water molecules in B-type state has one –OH pointing towards nanotube wall and the other –OH pointing to another water molecule, forming only one hydrogen bond. The ordered hexagonal structure is in

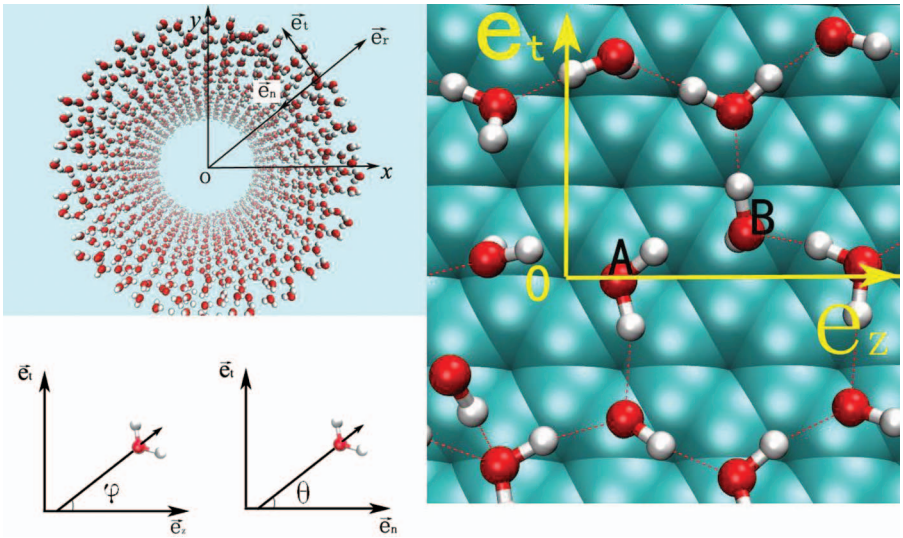

FIG. 4. Snapshot of the ice-like water shell (ice nanotube) near the nanotube wall (top left) and a schema for φ and θ (bottom left), where φ is the angle formed between the projection of a water dipole orientation onto the e_t-e_z plane (the tangent surface) and the z direction, and θ is the angle formed between the projection of a water dipole orientation onto the x-y plane (cross section) and the normal to the tangent plane to the nanotube wall surface. The structure of the ice-like water monolayer on the nanotube wall together with the hydrogen bonds between neighboring water molecules (right).

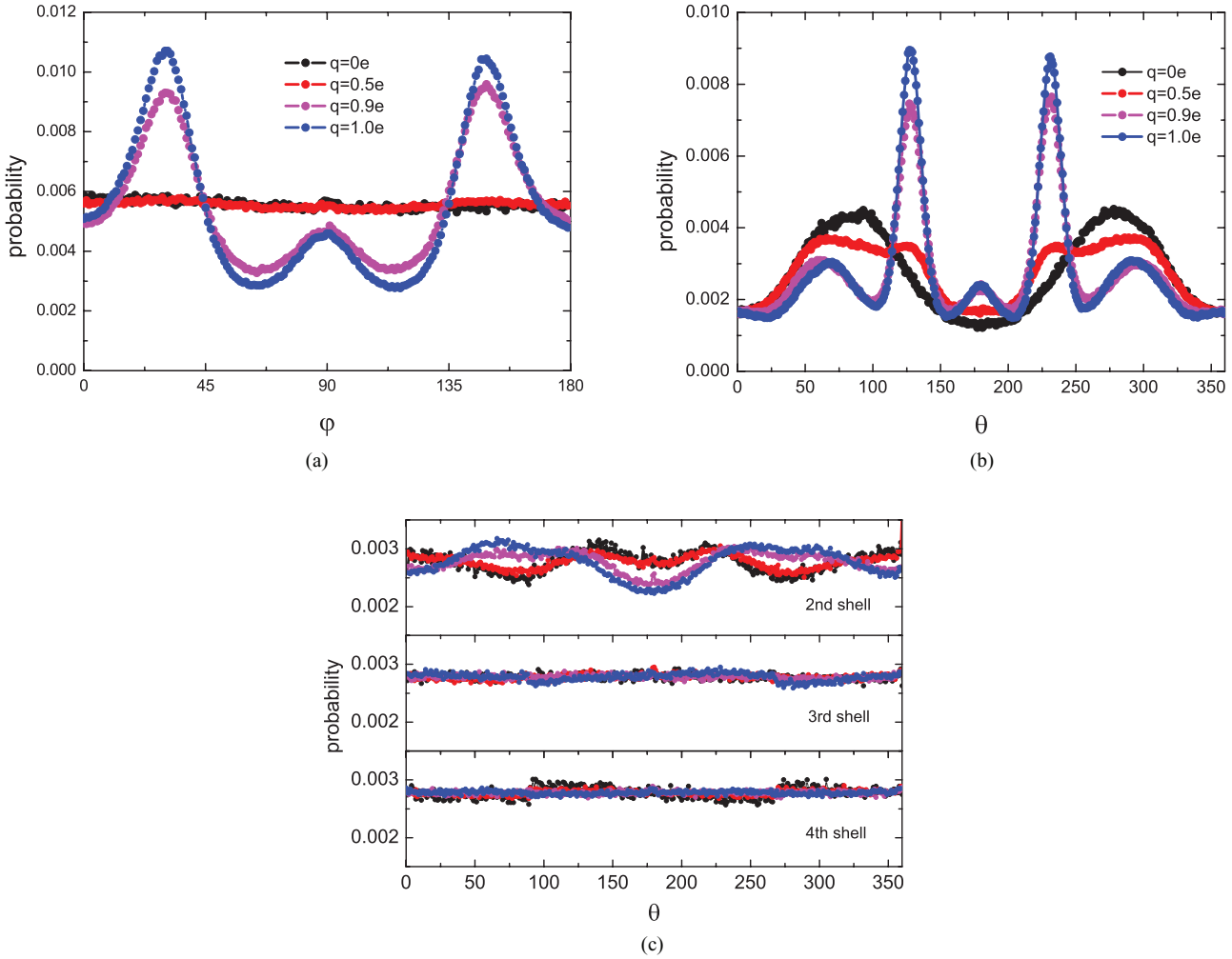

FIG. 5. (a) Probability distribution of the angle φ. (b) Probability distribution of the angle θ. (c) Probability distribution of the angle θ for 2nd, 3rd, and 4th shells.

agreement with our previous results,[17,21] which is further confirmed by the probability distribution of water dipole orientations. We introduce two angles φ and θ to describe the dipole orientation, where φ is the angle formed between the projection of a water dipole orientation onto the 2D surface by unwrapping the nanotube (the tangential plane to the nanotube wall) and the z direction, and θ is the angle formed between the projection of a water dipole orientation onto the cross section and the normal (the negative radial direction).

For neutral nanotube, φ is distributed uniformly, indicating that the water dipole orientations are random. However, for the charged nanotube, when $q > q_c$, there is a clear preference in the orientation of water dipoles, with three peaks at $\varphi = 30°$, 90°, and 150°, as shown in Fig. 4 (correspondingly, there are three other peaks at $\varphi = 210°$, 270°, and 330° due to symmetry, not shown in Fig. 4). These peaks correspond perfectly to the hexagonal 2D hydrogen-bond networks. We note that the peak at $\varphi = 90°$ is much lower than other peaks which is due to the fact that the 2D solid substrate was rolled into a nanotube along the $\boldsymbol{e}_t$ axis, not the z axis. It is known that the water molecules in the first monolayer near a charged plane (e.g., unwrapping the nanotube) tend to form 2D-ordered hexagonal configurations.[17,21] As the bond length deviates from 0.142 nm, the ordered water monolayer disappears and the preference of the water dipole orientations decreases.[17] For the same reason, the probability of $\varphi = 90°$ for the charged nanotube is lower than that for the charged plane. For all other water shells, no meaningful peaks were observed in our simulations, indicating that the structure of water molecules in the first shell is different from the other water shells.

Furthermore, the probability distribution of the water dipole orientation θ was calculated and shown in Figs. 5(b) and 5(c) for different q. For $\theta = 180°$, the water dipole orientation points directly towards the nanotube wall (i.e., normal to the wall). For neutral tube, it is clear that there are two relatively broad peaks near $\theta = 80°$ and 280° for the 1st shell. For $q > q_c$, there are five sharper peaks in the region $53° < \theta < 84°$, $113° < \theta < 142°$, $168° < \theta < 190°$, $198° < \theta < 247°$, and $276° < \theta < 307°$, respectively. The lower two peaks in the region $53° < \theta < 84°$ and $276° < \theta < 307°$ of the blue lines correspond to the water molecules in A-type state having both –OH vectors pointing towards the two neighboring water molecules. The two higher peaks near $\theta = 130°$ and 230° correspond to the water molecules in B-type state with one –OH vector pointing to another water molecule and the

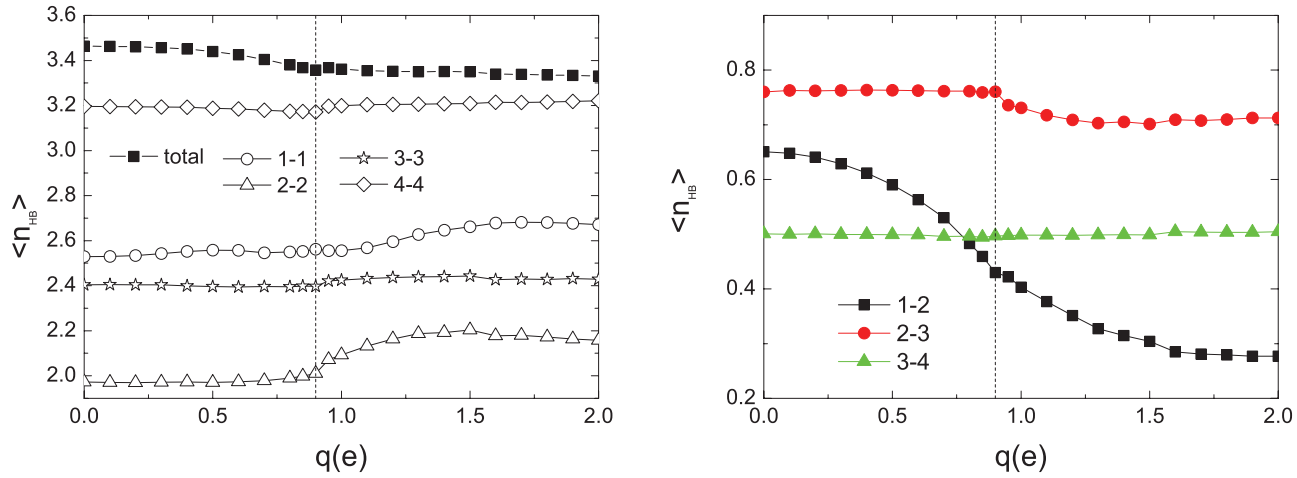

FIG. 6. Average number of hydrogen bonds formed by a water molecule in different shells and between shells with respect to q.

other –OH vector pointing towards the wall. The snapshot of the A-type and B-type water molecules is shown in Fig. 4. Different from our previous work,[21] one small peak around $\theta = 180^\circ$ is found for nanotube. This indicates that the hexagonal structure of water on nanotube wall is not as perfect as on a pure substrate plane. Figure 5(c) shows the probability distribution of θ for 2nd, 3rd, and 4th water layers. For 2nd shell, the orientation of the water dipole is affected by the charge on the wall. And in the other shells, the distribution is uniform, indicating that the influence of the charges upon the orientation of water dipoles is largely "screened."

We then computed average number of H-bonds formed by a water molecule in different shells and between shells with respect to q in order to better understand the effects of the ordered water monolayer near the wall on the abnormal diffusion of other inner water shells. The results are shown in Fig. 6. When $q < 0.9e$, the average number of H-bonds formed by a water molecule in all shells and between shells (2-3 and 3-4) remains almost constant. However, the most noticeable change is for the H-bonds between 1 and 2 shells, which decreases from 0.65 to 0.28 as q increases over the interval of 0.0-1.6e. The average number of H-bonds in the first shell increases about 0.15 for $q > 0.9e$, while the total H-bonds of each water molecule in the first shell decreases from 3.2 to 3.0 with q increasing to 1.6e. Note that when q is sufficiently large, for each water molecule in the first shell, there is approximately one occupied charge site to account for the electrostatic interactions from the charges on the nanotube. Half of the water molecules in the first shell bind to the charged nanotube wall mainly through attractive Coulomb interaction between their O atoms and the positive charges on the nanotube wall, while the other half bind to the wall through the strong electrostatic interactions between H atoms and the negative charges on the nanotube wall (the –OH vector pointing towards the wall). This can also be clearly seen in Fig. 4. Meanwhile, there is a significant decrease in the average number of H-bonds, 0.37 (from 0.65 to 0.28), between the second and first shell (2-1), resulting in weaker interactions for the water molecules in the second shell. Similarly, the number of H-bonds between the second and the third shell (2-3) also decreases slightly. Thus, the axial diffusion coefficient of the water molecules in the second shell increases. For the third shell, the number of H-bonds within this shell increases slightly, which partially compensate the small loss in-between the third and the second shells (when $q > 0.9e$). Both the H-bonds within the fourth shell and in-between the third and fourth shells are almost unchanged. We, thus, conclude that the slight increases of the axial diffusion coefficients of the water molecules in the third and fourth shells result from the "dragging" of the second shell.

IV. CONCLUSION

We have observed well-ordered ice-like hexagonal configurations of water molecules near the charged nanotube wall at the room temperature with molecular dynamics simulations. This striking phenomenon is attributed to a certain charge value and charge distribution that provides strong and specific Coulomb interactions. Moreover, simulation results suggest that this ice-like ordered hexagonal water monolayer ("ice nanotube") plays a key role in the diffusion behavior of inner water shells confined inside the nanotube. The axial diffusion coefficient of the first water monolayer near the wall monotonously decreases with the charge size on the nanotube; however, the average axial diffusion coefficients for the other water shells increase with q, when the charge q is above a certain threshold and the "ice nanotube" forms. There is a significant decrease in the average number of H-bonds between the water molecules in the second water shell and the first "ice nanotube" layer. This significant decrease in the number of inter-shells H-bonds results in much weaker interactions between the water molecules in the second shell and the "ice nanotube." The physical origin of this phenomenon lies in that the water molecules in the "ice nanotube" tend to form well ordered hexagonal configurations which lead to rare H-bond saturation for each water molecule.

ACKNOWLEDGMENTS

We would like to thank Haiping Fang, Seung-gu Kang, and Junxia He for helpful discussions. This work is partially supported by the National Natural Science Foundation

of China (NNSFC) under Grant No. 11005093, the Zhejiang Provincial Natural Science under Grant Nos. Y6100384 and Z6090556, and the Research Fund of Department of Education of Zhejiang Provincial under Grant No. Y201225965. R.Z. acknowledges the support from the IBM Blue Gene Science Program.

[1]M. J. Higgins, M. Polcik, T. Fukuma, J. E. Sader, Y. Nakayama, and S. P. Jarvis, Biophys. J. **91**, 2532 (2006).
[2]E. J. W. Wensink, A. C. Hoffmann, M. E. F. Apol, and H. J. C. Berendsen, Langmuir **16**, 7392 (2000).
[3]G. Cicero, J. C. Grossman, E. Schwegler, F. Gygi, and G. Galli, J. Am. Chem. Soc. **130**, 1871 (2008).
[4]P. Liu, X. Huang, R. Zhou, and B. J. Berne, Nature (London) **437**, 159 (2005).
[5]R. Zhou, X. Huang, C. J. Margulis, and B. J. Berne, Science **305**, 1605 (2004).
[6]B. J. Berne, J. D. Weeks, and R. Zhou, Annu. Rev. Phys. Chem. **60**, 85 (2009).
[7]J. Peon, S. K. Pal, and A. H. Zewail, Proc. Natl. Acad. Sci. U.S.A. **99**, 10964 (2002).
[8]A. Michaelides and K. Morgenstern, Nature Mater. **6**, 597 (2007).
[9]S. K. Pal and A. H. Zewail, Chem. Rev. **104**, 2099 (2004).
[10]S. H. Park and G. Sposito, Phys. Rev. Lett. **89**, 085501 (2002).
[11]H. Ogasawara, B. Brena, D. Nordlund, M. Nyberg, A. Pelmenschikov, L. G. M. Pettersson, and A. Nilsson, Phys. Rev. Lett. **89**, 276102 (2002).
[12]S. Meng, E. G. Wang, and S. Gao, Phys. Rev. B **69**, 195404 (2004).
[13]J. Carrasco, A. Hodgson, and A. Michaelides, Nature Mater. **11**, 667 (2012).
[14]F. Zaera, Chem. Rev. **112**, 2920 (2012).
[15]J. Hu, X. D. Xiao, D. F. Ogletree, and M. Salmeron, Science **268**, 267 (1995).
[16]M. James, S. Ciampi, T. A. Darwish, T. L. Hanley, S. O. Sylvester, and J. J. Gooding, Langmuir **27**, 10753 (2011).
[17]M. James, T. A. Darwish, S. Ciampi, S. O. Sylvester, Z. Zhang, A. Ng, J. J. Gooding, and T. L. Hanley, Soft Matter **7**, 5309 (2011).
[18]C. Wang, B. Zhou, P. Xiu, and H. Fang, J. Phys. Chem. C **115**, 3018 (2011).
[19]C. Wang, J. Li, and H. Fang, Rend. Fis. Acc. Lincei **22**, 5 (2011).
[20]C. L. Wang, H. J. Lu, Z. G. Wang, P. Xiu, B. Zhou, G. H. Zuo, R. Z. Wan, J. Hu, and H. P. Fang, Phys. Rev. Lett. **103**, 137801 (2009).
[21]B. Rotenberg, A. J. Patel, and D. Chandler, J. Am. Chem. Soc. **133**, 20521 (2011).
[22]A. Phan, T. A. Ho, D. R. Cole, and A. Striolo, J. Phys. Chem. C **116**, 15962 (2012).
[23]R. J. Mashl, S. Joseph, N. R. Aluru, and E. Jakobsson, Nano Lett. **3**, 589 (2003).
[24]X. Y. Zhou and H. J. Lu, Chin. Phys. **16**, 335 (2007).
[25]J. K. Holt, H. G. Park, Y. M. Wang, M. Stadermann, A. B. Artyukhin, C. P. Grigoropoulos, A. Noy, and O. Bakajin, Science **312**, 1034 (2006).
[26]K. Koga, G. T. Gao, H. Tanaka, and X. C. Zeng, Nature (London) **412**, 802 (2001).
[27]G. Hummer, J. C. Rasaiah, and J. P. Noworyta, Nature (London) **414**, 188 (2001).
[28]J. Li, X. Gong, H. Lu, D. Li, H. Fang, and R. Zhou, Proc. Natl. Acad. Sci. U.S.A. **104**, 3687 (2007).
[29]Y. Tu, P. Xiu, R. Wan, J. Hu, R. Zhou, and H. Fang, Proc. Natl. Acad. Sci. U.S.A. **106**, 18120 (2009).
[30]P. Das and R. Zhou, J. Phys. Chem. B **114**, 5427 (2010).
[31]P. Xiu, Y. Tu, X. Tian, H. Fang, and R. Zhou, Nanoscale **4**, 652 (2012).
[32]P. Xiu, Z. Yang, B. Zhou, P. Das, H. Fang, and R. Zhou, J. Phys. Chem. B **115**, 2988 (2011).
[33]G. Che, B. B. Lakshmi, E. R. Fisher, and C. R. Martin, Nature (London) **393**, 346 (1998).
[34]A. Barati Farimani and N. R. Aluru, J. Phys. Chem. B **115**, 12145 (2011).
[35]A. Striolo, Nano Lett. **6**, 633 (2006).
[36]Y. C. Liu, Q. Wang, T. Wu, and L. Zhang, J. Chem. Phys. **123**, 234701 (2005).
[37]Y. C. Liu and Q. Wang, Phys. Rev. B **72**, 085420 (2005).
[38]Y. C. Liu, J. W. Shen, K. E. Gubbins, J. D. Moore, T. Wu, and Q. Wang, Phys. Rev. B **77**, 125438 (2008).
[39]S. Joseph and N. R. Aluru, Nano Lett. **8**, 452 (2008).
[40]T. Susi, G. Lanzani, A. G. Nasibulin, P. Ayala, T. Jiang, T. Bligaard, K. Laasonen, and E. I. Kauppinen, Phys. Chem. Chem. Phys. **13**, 11303 (2011).
[41]C. A. Dyke and M. James, J. Am. Chem. Soc. **125**, 1156 (2003).
[42]A. A. Mamedov, N. A. Kotov, M. Prato, D. M. Guldi, J. P. Wicksted, and A. Hirsch, Nature Materials **1**, 190 (2002).
[43]H. Li, M. Eddaoudi, M. O'Keeffe, and O. M. Yaghi, Nature **402**, 276 (1999).
[44]C. Oostenbrink, A. Villa, A. E. Mark, and W. F. Van Gunsteren, J. Comput. Chem. **25**, 1656 (2004).
[45]J. Ma, A. Michaelides, D. Alfe, L. Schimka, G. Kresse, and E. G. Wang, Phys. Rev. B **84**, 033402 (2011).
[46]E. M. Kotsalis, J. H. Walther, and P. Koumoutsakos, Int. J. Multiphase Flow **30**, 995 (2004).
[47]I. Hanasaki and A. Nakatani, J. Chem. Phys. **124**, 144708 (2006).